atmosphere-land models to the ERA-40 reanalysis. Perturbed atmospheric initial conditions are obtained by taking the nudged analysis from earlier and later 3 hour periods around the first of each month.

The POAMA system exhibits high skill (anomaly correlation exceeding 0.7) for predicting heat content anomaly throughout the equatorial central and east Pacific at lead times beyond 6 months (not shown), which is reflective of the ability of the POAMA system to predict ENSO. High skill is also evident off of the equator in the far west Pacific (presumably associated with the slow westward propagating Rossby waves generated during ENSO) and on the northwest shelf of Australia. This high skill on the northwest shelf reflects the ability to predict the oceanic teleconnection of ENSO from the Pacific, through the Indonesian throughflow. This is demonstrated in Figure 2b, which shows the correlation of the observed HCNW with the predicted heat content over the tropical Pacific and Indian Oceans at a 6 month lead time. The resemblance with the observed heat content anomaly that is associated with Fremantle sea level variation (Figure 2a) is outstanding.

Skill of predicting HCNW and the Niño4 SST index is summarized in Figure 4. Except at short lead time, the skill is essentially identical for both Niño4 and HCNW. The anomaly correlation for both remains high (>0.75) to 9 month lead time and readily beats persistence. In light of the tight coupling between HCNW and FLSA, skilful seasonal prediction of the Leeuwin Current appears to be as feasible as prediction of ENSO.

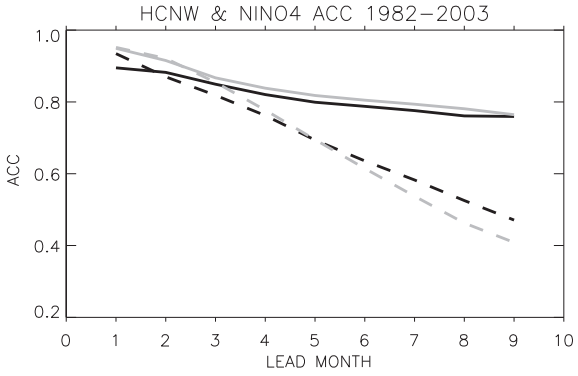

Fig. 4 Anomaly correlation for Nino4 SST index (grey) and HCNW (black) as a function of forecast lead time. Persistence (in dashed lines) is shown for reference. Correlation is computed using ensemble mean of forecasts for the period 1982-2003.

Concluding Remarks

This study is part of an ongoing investigation into seasonal predictability of the marine environment of Western Australia. Future work will include downscaling of the dynamical model predictions of heat content to direct prediction of Leeuwin Current strength, evaluation of the value added by prediction of heat content on the northwest shelf over that of simply predicting ENSO in the Pacific, and investigation of the role of coupled processes in the Indian Ocean for contributing to variability and predictability of the Leeuwin Current.

Acknowledgement

Ming Feng kindly provided his time series of Fremantle sea level anomaly. Support for this work was provided in part from the Western Australian Marine Science Institution (WAMSI) www.wamsi.org.au .

References

Clarke, A.J., and X. Liu, 1994: Interannual sea level in the northern and eastern Indian Ocean. *J. Phys., Oceanogr.*, **24**, 1224-1235.

Feng, M., G. Meyers, A. Pearce, S. Wijffels, 2003: Annual and Interannual Variations of the Leeuwin Current at 32°S, *J. Geophys. Res.*, **108(11)**, 3355, doi:10.1029/2002JC001763.

Godfrey, J. S., and K. R. Ridgway, 1985: The large-scale environment of the poleward-flowing Leeuwin Current, Western Australia: Longshore steric height gradients, wind stresses, and geostrophic flow, *J. Phy. Ocean.*, **15**, 481-495.

Legeckis, R., and G.R. Cresswell, 1981: Satellite observations of sea surface temperature fronts off the coast of western and southern Australia. *Deep-Sea Res*. **28A**, 297-306.

Pearce, A. F., and B. F. Phillips, 1988: ENSO events, the Leeuwin Current and larval recruitment of the western rock lobster, *J. Cons. Int. Explor. Mer.*, **45**, 13-21.

Reason, C.J.C., D. Gamble, and A.F. Pearce, 1999: the Leeuwin Current in the Parallel Ocean Climate Model and applications to regional meteorology and fisheries. *Meteorol. Appl.* **6,** 211-225.

Smith, R.L. A. Huyer, J.S. Godfrey, and J. Church, 1991: The Leeuwin Current off Western Australia, 1986-1987. *J. Phys., Oceanogr.*, **21**, 323-345.

Wiffels, S.and G. Meyers, 2003: An intersection of oceanic wave guides: Variability in the Indonesian throughflow region. *J. Phys. Oceanogr*., **34,** 1232-1253.

Zhong, A., H.H. Hendon, and O. Alves, 2005: Indian Ocean variability and its association with ENSO in a global coupled model. *J. Climate*, **18**, 3634-3649.

Seasonal Rainfall Anomalies over Western Australia Forced by Indian Ocean SST – Scope for Improved Forecasting

Ummenhofer, C.C.,[1], A. S. Gupta[1], M. J. Pook[2], and M. H. England[1]
[1] Climate and Environmental Dynamics Laboratory, School of Mathematics and Statistics, University of New South Wales, Sydney, Australia. [2] CSIRO Marine and Atmospheric Research, Hobart, Tasmania, and Wealth from Oceans National Research Flagship, CSIRO, North Ryde, New South Wales, Australia
Corresponding author: C.Ummenhofer@unsw.edu.au

Introduction

On seasonal to interannual timescales, it is generally assumed that the ocean's role in modulating mid-latitude precipitation is minor relative to internal atmospheric variability. This is in contrast to the well-established view that air-sea coupling is of paramount importance in the tropics. In this study, we use atmospheric general circulation model (AGCM) simulations to assess the way in which Indian Ocean SST anomalies modulate mid-latitude precipitation across western regions of Australia. Our study represents an extension of previous work by England et al. (2006) who find that, in the observed record, extremes in southwest Western Australia (SWWA) rainfall are associated with characteristic SST patterns and changes in the large-scale atmospheric circulation across the Indian Ocean. Here, we show that these SST composite patterns can significantly affect SWWA and Western Australia precipitation in ensemble sets of AGCM simulations. We also propose a mechanism for the observed rainfall shifts due to changes in the large-scale general circulation (Ummenhofer et al., 2007).

Model and experimental setup

A set of ensemble experiments is conducted with the NCAR Community System Model, version 3 (CCSM3; Collins et al., 2006), run in uncoupled atmosphere-only mode. The atmospheric component of CCSM3, the Community Atmosphere Model (CAM3; Hurrell et al., 2006) uses a spectral dynamical core, T42 horizontal resolution (~2.8° latitude/longitude), and 26 vertical levels. Ummenhofer et al. (2007) assess the model's performance over the Indian Ocean and Australian region on seasonal to interannual timescales and demonstrate the model's suitability for the present study.

An 80-year integration forced by a 12-month SST climatology (Hurrell et al., 2006) represents the control experiment (CNTRL). Two sets of perturbation experiments are carried out where anomalous SST patterns are superimposed onto the climatology. These perturbations are derived from composites of observed average monthly SST anomalies for years defined as being anomalously dry/wet over SWWA (30°-35°S, 115°-120°E) by England et al. (2006), i.e. exceeding ±1 standard deviation in their rainfall time-series. The resulting monthly-varying SST anomalies are scaled by a factor of three in an attempt to excite a clearer atmospheric response from the inherently noisy atmosphere. Despite this scaling the applied magnitude of SST perturbations is not unrealistic, with certain years showing similar SST anomaly magnitudes (for further details see Ummenhofer et al., 2007). All of the "dry-year" (PDRY) and "wet-year" (PWET) perturbation runs start from early January from a variety of years spanning the control run. The ensemble sets consist of 60 one-year integrations for each of the PDRY and PWET scenarios.

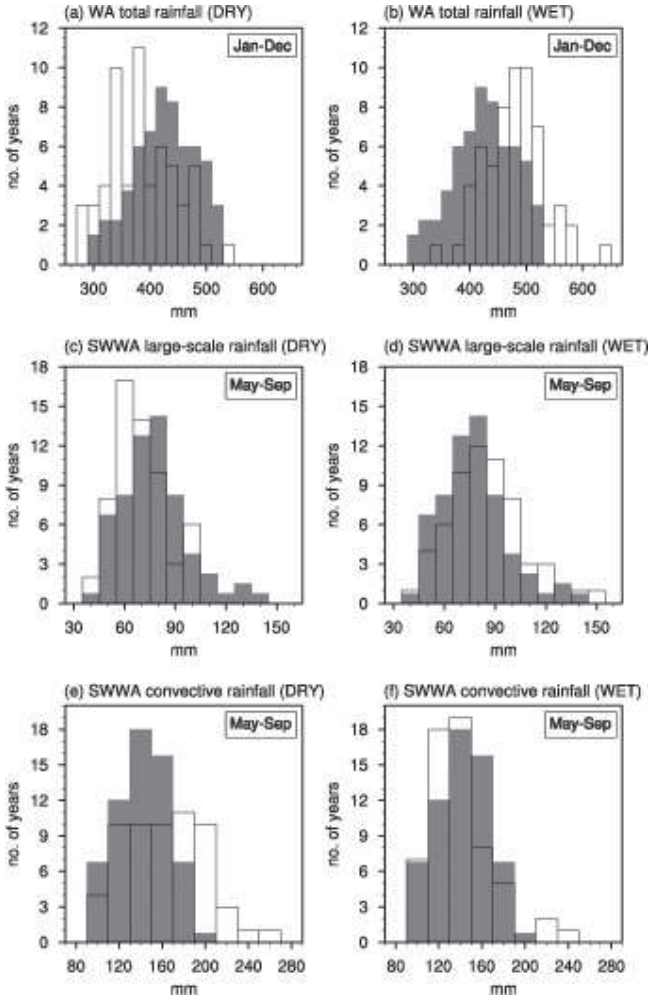

Figure 1. Frequency distribution of (a, b) total rainfall spatially averaged across WA; (c, d) large-scale and (e, f) convective rainfall spatially averaged across SWWA; cumulative rainfall amount (in mm) summed over the months indicated for PDRY (left) and PWET (right) cases. The shaded gray rainfall distribution represents the CNTRL (normalized to the number of ensemble members in PDRY/PWET), while PDRY and PWET are indicated with black outlines. The following significance levels hold, as determined by a Mann-Whitney test: (a) 99%, (b) 99%, (c) 99%, (d) 95%, (e) 99%. (adapted from Ummenhofer et al., 2007).

Rainfall shifts

The impact of the modified SST is assessed for precipitation across western regions of Australia. Fig. 1 shows the rainfall frequency distribution across the ensemble members in PDRY and PWET relative to the CNTRL. The total annual precipitation is spatially averaged over the region of Western Australia (WA; 21°-35°S, 115°-130°E). This area excludes the tropical north of the state dominated by monsoonal rainfall and integrates across coastal regions with predominant winter rainfall and dry regions farther inland with a more uniform annual rainfall distribution. The model results indicate a shift in the distribution towards lower (higher) rainfall amounts in the PDRY (PWET) case relative to the CNTRL (Fig. 1a, b; significant at the 99% confidence level).

The model distinguishes between large-scale and convective components of precipitation, providing a first insight into the likely causes for the simulated rainfall shifts. Over WA, these components reinforce each other and are of opposite sign for PDRY and PWET (Fig. 1a, b). This contrasts with the rainfall breakdown for the smaller area of SWWA (30°-35°S, 115°-120°E), where the two components are not necessarily of the same sign. As a result, large-scale and convective components are presented separately over the predominant SWWA rainfall season May-September (Fig. 1c-f). The large-scale rainfall distribution is shifted towards low (high) rainfall amounts for PDRY (PWET) relative to the CNTRL (Fig. 1c, d). A disproportionate decrease (increase) in the number of ensemble members receiving in excess of 100 mm (summed for May-September) is observed for PDRY (PWET). Only 5% of winters (May-September) in the PDRY case receive >100 mm, while this occurs in 13% of winters in the CNTRL and 22% in the PWET case. The frequency distribution for convective precipitation over SWWA shows less consistent shifts (Fig. 1e, f). Significantly more ensemble members receive high convective precipitation for PDRY relative to the CNTRL, while no significant change is recorded for PWET.

Atmospheric dynamics

To understand the mechanisms responsible for the observed shifts in precipitation, we investigate changes in the atmospheric general circulation induced by the SST perturbations. We focus on the May-September period, as most of the SWWA rain falls during these months (~70% of annual total) and the anomalies of various atmospheric variables are particularly strong during the winter season (Ummenhofer et al., 2007).

The SST anomalies during dry/wet years form a characteristic dipole pattern which is distinct in location and temporal evolution from previous definitions of dipoles in the Indian Ocean (e.g., Saji et al., 1999; Behera and Yamagata, 2001). A pole of cold (warm) SST anomalies develops in the eastern Indian Ocean over the northwest shelf of Australia (named P1) at the same time as warm (cold) anomalies form in the central subtropical Indian Ocean (named P2) for PDRY (PWET),

reaching maximum magnitudes in late winter/early spring (Fig. 2a, b). Atmospheric thickness anomalies (1000-500 hPa) of the same sign and position as the underlying SST anomalies at P1 and P2 develop in the perturbation experiments, intensifying towards late winter and extending across southern regions of Australia (Fig. 2c, d). This leads to a weakening (intensification) of the meridional thickness gradient and the subtropical jet during the winter in PDRY (PWET), with a coincident easterly (westerly) anomaly in the thermal wind over southern regions of Australia. The offshore (onshore) wind anomalies over SWWA (Fig. 2e, f) thus contribute to the reduction (increase) in large-scale rainfall. In observations, Ansell et al. (2000) similarly associate variations (and trends) in SWWA rainfall with modulations in the subtropical high pressure belt and a shift of the circumpolar trough. However in their study, links with Indian and Pacific Ocean SST are weak compared to the variability of the large-scale atmospheric circulation, while we demonstrate that the reorganization in the general atmospheric circulation can arise as a result of the changed SST fields over the Indian Ocean.

A measure of the baroclinic stability in the atmosphere, and hence its disposition towards developing rain-bearing low pressure systems, is provided by the Eady growth rate. A reduction (increase) in the Eady growth rate (Fig. 2g, h) indicates a lower (higher) formation rate of baroclinic instabilities over southern and western regions of Australia during PDRY (PWET), consistent with the large-scale rainfall changes. Hope et al. (2006) also link trends in baroclinicity and reduced frequency of passing troughs across the region with the observed rainfall decrease over SWWA. Here, we demonstrate that such changes can be driven by anomalous SST patterns over the Indian Ocean. The vertical thermal structure overlying warm SST anomalies at P2 in the central subtropical Indian Ocean in PDRY favors localized increases in convective activity, as seen in the increase in convective rainfall over SWWA and the reduction in large-scale rainfall. The asymmetry in convective rainfall response does not manifest itself in the rainfall distribution for WA, most likely due to the fact that with increasing distance inland, the impact of the warm SST at P2 giving rise to localized convective upward motion and enhanced convective rainfall in SWWA during PDRY is averaged away. On the other hand, both the circulation and thermal anomalies in PWET enhance widespread ascent of moist air masses associated with frontal movement, as evidenced by increases in large-scale precipitation in that ensemble set for both the SWWA and WA regions.

In summary, we have demonstrated that the Indian Ocean SST anomalies associated with dry/wet years over WA can themselves force significant anomalies in rainfall over the region. The SST anomaly fields involve both tropical and subtropical perturbations, combining to drive changes in atmospheric thickness, thermal winds, baroclinicity, and moisture advection onto the Western Australian coast. Future work will assess the relative roles of the tropical and subtropical SST anomalies in driving these rainfall changes and the lead times of predictability that may be involved.

References

Ansell, T.J., C.J.C. Reason, I.N. Smith, and K. Keay, 2000: Evidence for decadal variability in southern Australian rainfall and relationships with regional pressure and sea surface temperature. *Int. J. Climatol.*, **20**, 1113-1129.

Behera, S.K. and T. Yamagata, 2001: Subtropical SST dipole events in the southern Indian Ocean. *Geophys. Res. Lett.*, **2**8, 327-330.

Collins, W.D., and Co-authors, 2006: The Community Climate System Model version 3 (CCSM3). *J. Climate*, **19**, 2122-2143.

England, M.H., C.C. Ummenhofer, and A. Santoso, 2006: Interannual rainfall extremes over southwest Western Australia linked to Indian Ocean climate variability. *J. Climate*, **19**, 1948-1946.

Hope, P.K., W. Drosdowsky, and N. Nicholls, 2006: Shifts in the synoptic systems influencing southwest Western Australia. *Clim. Dyn.*, **26**, 751-764.

Hurrell, J.W., J.J. Hack, A.S. Phillips, J. Caron, and J. Yin, 2006: The dynamical simulation of the Community Atmosphere Model version 3 (CAM3). *J. Climate*, **19**, 2162-2183.

Saji, N.H., B.N. Goswami, P.N. Vinayachandran, and T. Yamagata, 1999: A dipole mode in the tropical Indian Ocean. *Nature*, **401**, 360-363.

Ummenhofer, C.C., A. Sen Gupta, M.J. Pook, and M.H. England, 2007: Anomalous rainfall over southwest Western Australia forced by Indian Ocean sea surface temperatures. *J. Climate*, submitted.

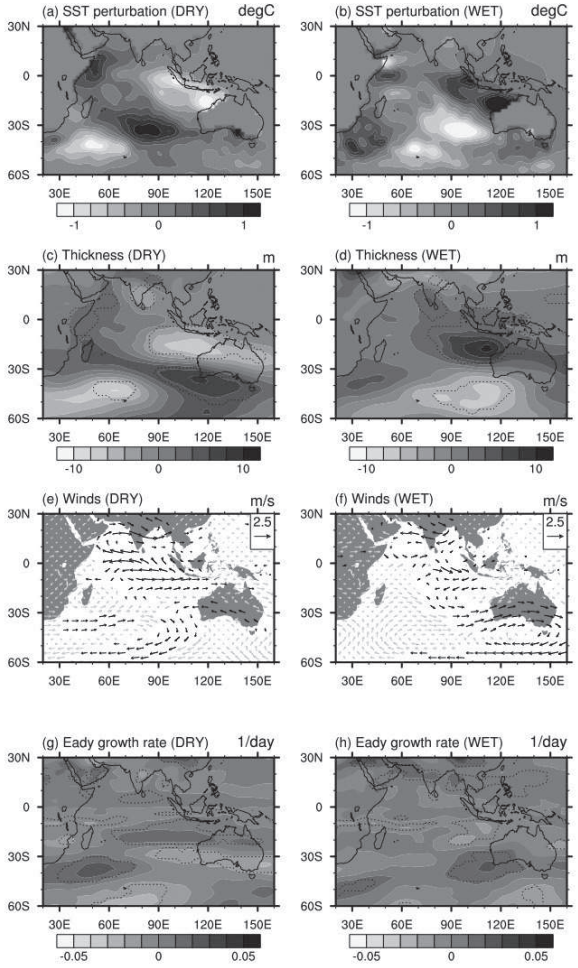

Figure 2. (a, b) SST perturbation (in °C), (c, d) thickness anomalies (in m for 1000-500 hPa), (e, f) wind anomalies at 500 hPa (in m s^{-1}), and (g, h) anomalies in Eady growth rate (in day^{-1}) averaged over the May-September period for the PDRY (left) and PWET (right) case, relative to the CNTRL. Dashed lines in (c, d, g, h) and black arrows in (e, f) indicate significant anomalies at the 90% confidence level as estimated by a two-tailed t-test. (adapted from Ummenhofer et al., 2007).